frontiers | Frontiers in Earth Science

TYPE Original Research
PUBLISHED 14 June 2023
DOI 10.3389/feart.2023.1204742

OPEN ACCESS

EDITED BY
Mohamed Ahmed,
Texas A&M University Corpus Christi,
United States

REVIEWED BY
Karem Abdelmohsen,
Western Michigan University,
United States
Abotalib Farag,
University of Southern California,
United States

*CORRESPONDENCE
Mohamed Abdelfattah,
mohamed_abdelfatah@sci.psu.edu.eg

RECEIVED 12 April 2023
ACCEPTED 31 May 2023
PUBLISHED 14 June 2023

CITATION
Abdelfattah M, Abdel-Aziz Abu-Bakr H, Aretouyap Z, Sheta MH, Hassan TM, Geriesh MH, Shaheen SE-D, Alogayell HM, M. EL-Bana EM and Gaber A (2023), Mapping the impacts of the anthropogenic activities and seawater intrusion on the shallow coastal aquifer of Port Said, Egypt.
Front. Earth Sci. 11:1204742.
doi: 10.3389/feart.2023.1204742

Mapping the impacts of the anthropogenic activities and seawater intrusion on the shallow coastal aquifer of Port Said, Egypt

Mohamed Abdelfattah[1]*, Heba Abdel-Aziz Abu-Bakr[2], Zakari Aretouyap[3], Mariam Hassan Sheta[4], Taher Mohammed Hassan[2], Mohamed H. Geriesh[5], Shams El-Din Shaheen[1], Haya M. Alogayell[6], Eman Mohamed M. EL-Bana[6] and Ahmed Gaber[1]

[1]Geology Department, Faculty of Science, Port Said University, Port Said, Egypt, [2]National Water Research Centre, Research Institute for Groundwater, Cairo, Egypt, [3]Department of Architecture and Engineering Art, Institute of Fine Arts, University of Dschang, Foumban, Cameroon, [4]Environmental Sciences Department, Faculty of Science, Port Said University, Port Said, Egypt, [5]Geology Department, Faculty of Science, Suez Canal University, Ismailia, Egypt, [6]Geography Department, College of Arts, Princess Nourah Bint Abdulrahman University, Riyadh, Saudi Arabia

The quality and quantity of groundwater resources have been continuously deteriorating as a result of anthropogenic activities and their excessive usage. This has intensified seawater intrusion, particularly in the coastal area of Egypt. The management of this issue and preventing ongoing groundwater contamination are crucial responsibilities. Thus, an integrated strategy using remote sensing, geophysical technique, and hydrogeochemical analysis is used in this work to identify the causes of degradation and evaluate their impacts on the groundwater quality in East Port Said, Egypt. The following points were identified: 1) Remote sensing analysis between 1984 and 2015 showed an increase in anthropogenic activities, such as the construction of fish farms and vegetation, which became their areas of 12.5 and 37.8 km^2 respectively. 2) Field observations demonstrated that the groundwater resources are being overexploited and it is expected that these human activities could have an impact on the groundwater quality. 3) The results of the resistivity approach indicated that sand and clay constitute the underlying layers and the shallow subsurface strata contain a high concentration of saline water. As a result, the aquifer is vulnerable to seawater intrusion due to its homogeneity. 4) Nineteen samples of groundwater were collected from the shallow Quaternary aquifer and the hydrochemical characteristic of the samples was identified. The hydrochemical analysis showed that the groundwater across the research area is of the Na-Cl water type and is highly saline (from 7,558 to 23,218 mg/L). By integrating the aforementioned techniques, it is evident that the research region is affected by anthropogenic activities as well as seawater intrusion on groundwater quality. These results serve as a solid base for further research on groundwater-surface water interactions and the evaluation of possible sources of contamination in the shallow aquifers under stress from anthropogenic activity in such environments.

KEYWORDS

coastal aquifer, Port Said, Egypt, groundwater quality, over-pumping, seawater intrusion

1 Introduction

Developments in land use land cover (LULC) are among the most vital factors to take into account change in investigations (Houghton, 1994; Lambin, 1997; Loveland et al., 2000; Brown et al., 2014; Chen et al., 2015). The expression "land use" refers to how humans exploit and use land resources, such as through urbanization and agriculture (Pielke Sr et al., 2002; Turner et al., 2014). These practices could result in excessive use of potentially harmful chemicals in agriculture, ineffective land use, improper sanitation, and excessive water consumption, all of which would be detrimental to groundwater quality (Mukherjee and Singh, 2021; Pal et al., 2022; Singh et al., 2022). Therefore, the groundwater quality of the shallow unconfined aquifers is closely related to the surface human activities which are reflected in LULC (Pielke Sr et al., 2002; Turner et al., 2014; Prabhakar and Tiwari, 2015).

Globally, groundwater contamination caused by LULC changes is a significant environmental issue. For example, Okinawa Island located in Japan is a region of concern for groundwater contamination caused by human activity such as agricultural activity is dominant (Ripken et al., 2021; Yoshihara et al., 2023). Another instance is southern China, a typical manufacturing region with an extensive record of producing and recycling various heavy metals, which poses a serious hazard to groundwater resources (Tang et al., 2023). Other locations around the world, such as the Trans-Pecos region in Texas (Robertson et al., 2017), the Shabestar basin in Iran (Ranjpisheh et al., 2018), and the Monte Desert in Argentina (Gebrehiwot et al., 2011), have provided evidence of these impacts.

In many arid/hyper-arid regions where surface water supplies are insufficient, groundwater is an essential resource for development (such as the building of new communities and agricultural expansion) (Khalil et al., 2021). There have been many mega-projects established throughout the Middle East and North Africa (MENA) region, including irrigation activities in Saudi Arabia (Elhadj, 2004), Syria (Haddad et al., 2008), Libya (Shaki and Adeloye, 2006), Iran (Farshad et al., 2002). In addition to the numerous projects already established throughout Egypt, whether they are in the delta (Khalil et al., 2015), and the coastal area (Abdelfattah et al., 2023; Gamal et al., 2023). Specific Egyptian

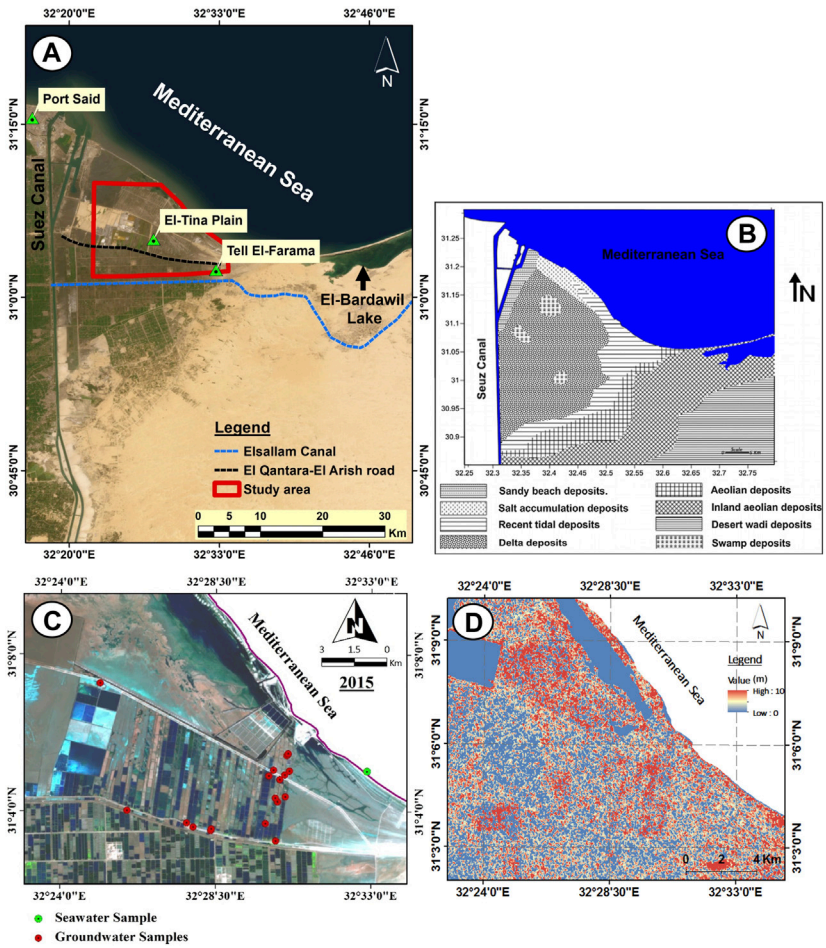

FIGURE 1
(A) Composite false color of Landsat-8 image (7, 5, 4 for RGB) shows location map of the study area related to Port Said city, **(B)** Surface geological map of the study area (Geological Survey of Egypt (GSE), 1992), **(C)** Digital elevation model (DEM) of the study area and **(D)** Map showing the locations of the groundwater and surface water samples that were collected.

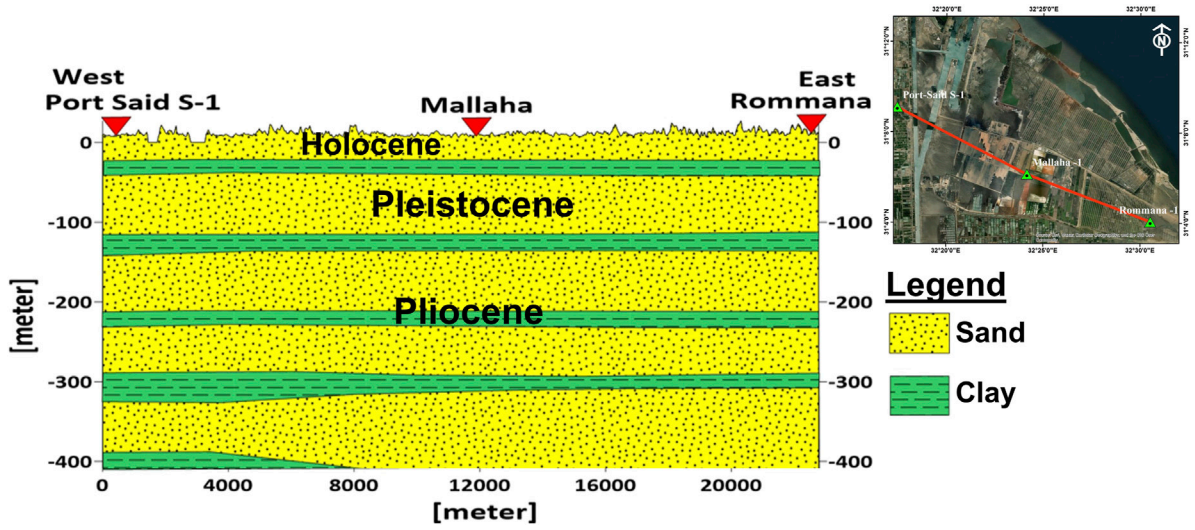

FIGURE 2
Subsurface hydrogeological cross-section.

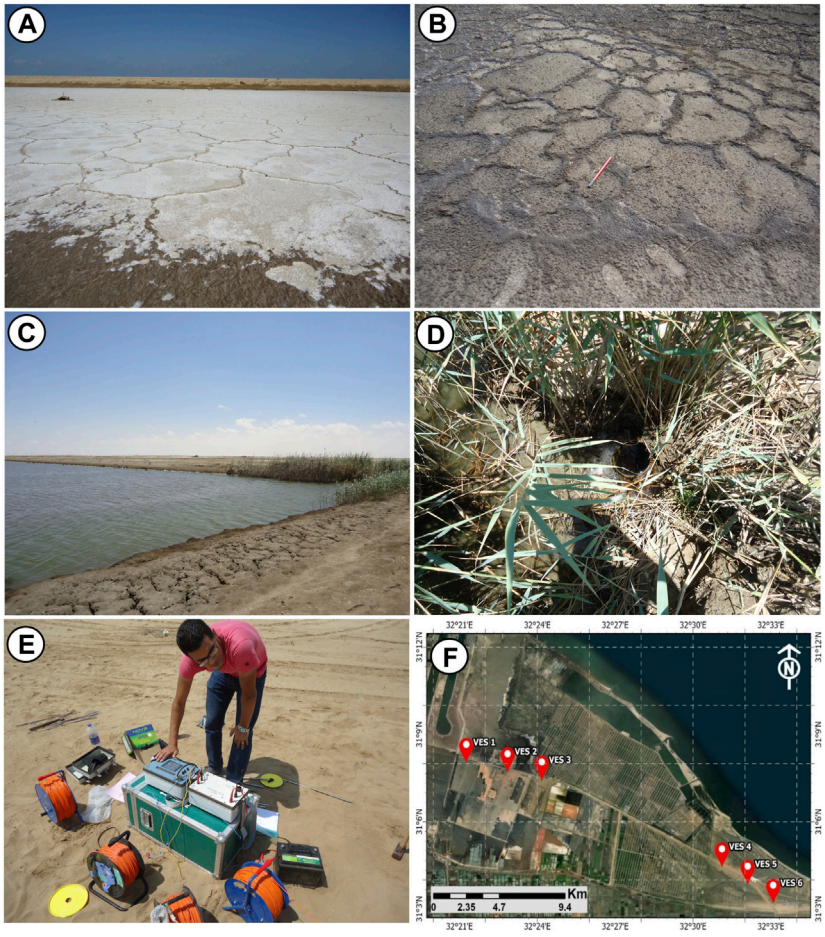

FIGURE 3
Surface features during site investigation within the study area such as **(A)** Sabkha, **(B)** Clay, **(C)** Fish farms, **(D)** Vegetation **(E)** Geophysical survey using Syscal R-2 system **(F)** Map shows the locations of resistivity soundings in the study area.

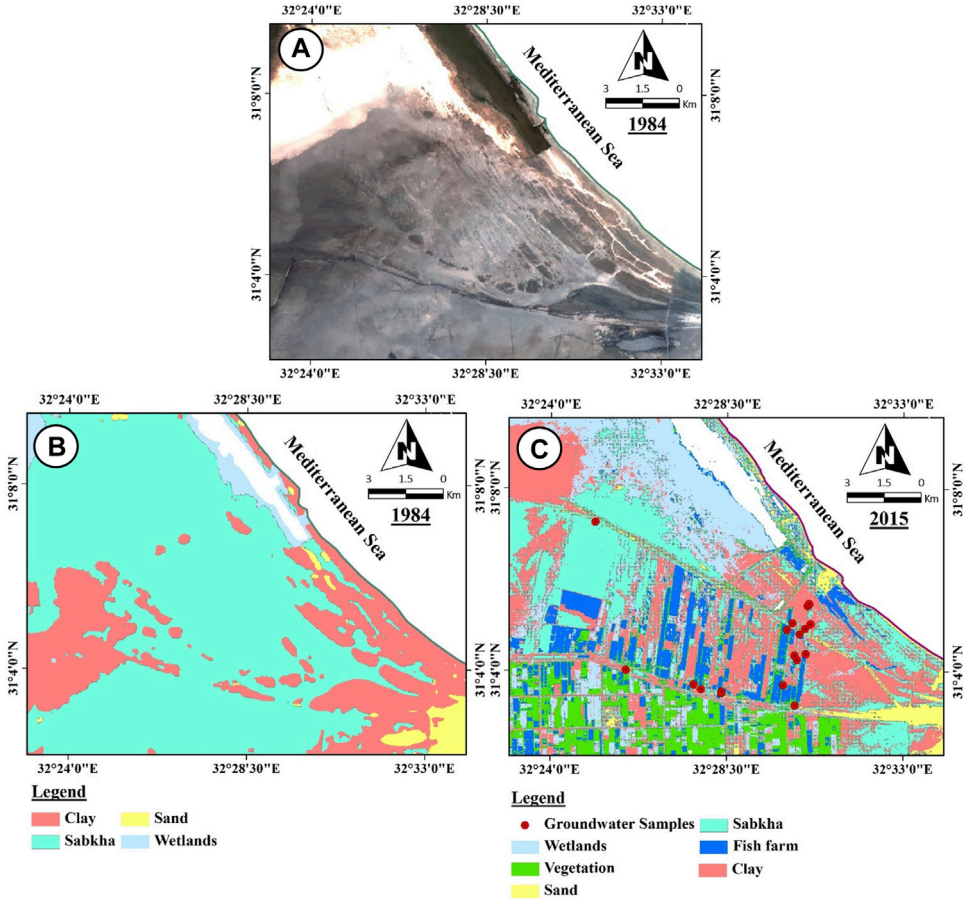

FIGURE 4
Drastic change observed in LU/LC along the study area; **(A)** Landsat-5 image of East Port Said in 1984, **(B)** Landcover units map of East Port Said in 1984, and **(C)** Landcover units map of East Port Said in 2015.

regions are suffering from groundwater stress caused by human activity, which has resulted in a deterioration in water quality (Saber et al., 2022; El-Aassar et al., 2023).

Changes in LULC may have a detrimental effect on groundwater quality because, for instance, thick unsaturated zones can act as a storage for salts that have gathered over a long time and can be discharged into underlying aquifers (Salem et al., 2015; Chávez et al., 2016). Increased groundwater abstraction and the addition of new sources of recharge are two common ways that agricultural developments affect groundwater quantity and quality (Switzman et al., 2015). This is particularly problematic for shallow aquifer systems. Consequently, the significant disposal of irrigation return, which is partially enriched with the residues of the utilized fertilizers, has had an impact on the water quality indices. Furthermore, the growing population results in a wide range of anthropogenic activities, such as the development of transportation systems, the generation of domestic waste in homes, the discharge of sewage sludge from nearby urban areas, and the dispersion of potentially toxic substances in the soil and water (Hegazy et al., 2020). Recent studies have investigated extensively the hydrologic response to changes in LCLU in terms of runoff dynamics (Napoli et al., 2017; El-Saadawy et al., 2020), groundwater temperature in shallow aquifers (Taylor and Stefan, 2009), water balance (Baker and Miller, 2013), shallow groundwater level fluctuation (Moukana et al., 2013), and groundwater pollution (Narany et al., 2014; Hegazy et al., 2020).

Land use changes have a considerable impact on the Nile Delta system in Egypt, leading the delta floodplain to considerably recede (Rateb and Abotalib, 2020). This exposes the Nile Delta aquifers to saltwater intrusion and groundwater degradation. Seawater intrusion is another factor that affects water quality in coastal regions around the world (Ahmed et al., 2013; Chidambaram et al., 2014; Abdalla et al., 2015). The over-extraction of groundwater and climate change, namely, seawater level rise, are the aggravating factors (Werner, 2010). Usually, the excessive extraction of water from the aquifer reduces the groundwater pressure and increases the lateral movement of seawater toward the land (Abdalla, 2016; Aretouyap et al., 2020). A significant number of water-intensive human activities are situated in the Egyptian coastal region, which is undergoing significant demographic, environmental, economic, and social changes (De Filippis et al., 2016).

Various strategies can be used to effectively manage water resources in coastal areas (Polemio and Zuffianò, 2020). To identify the saline contamination, hydrochemical methods can be employed to measure variables including electrical conductivity,

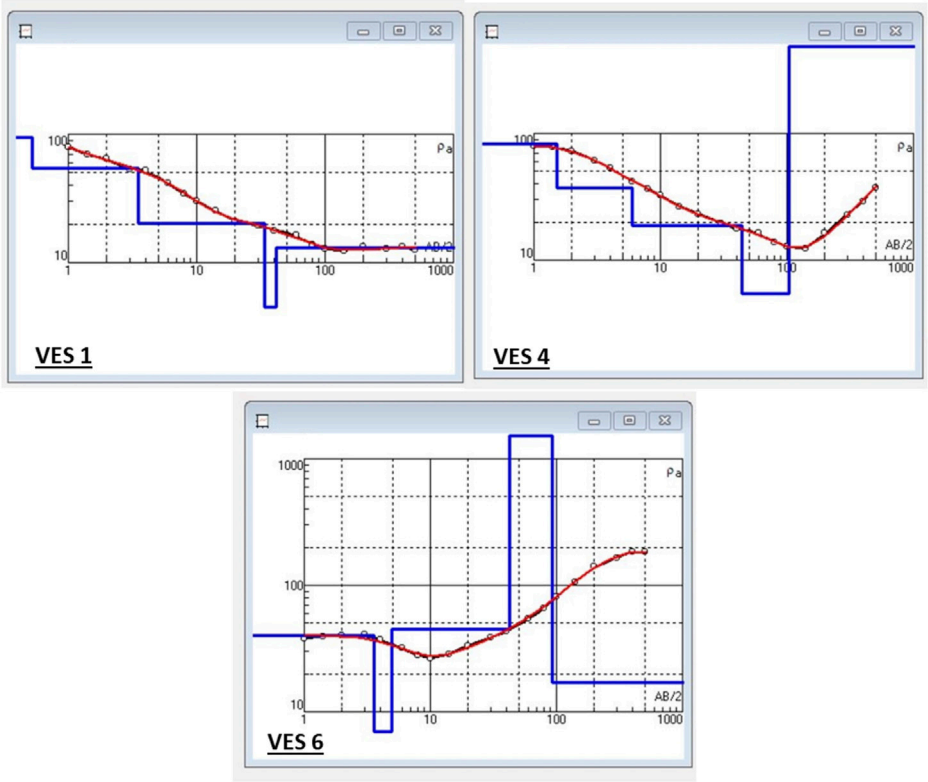

FIGURE 5
Examples of the processed resistivity soundings: VES1, VES4, and VES 6.

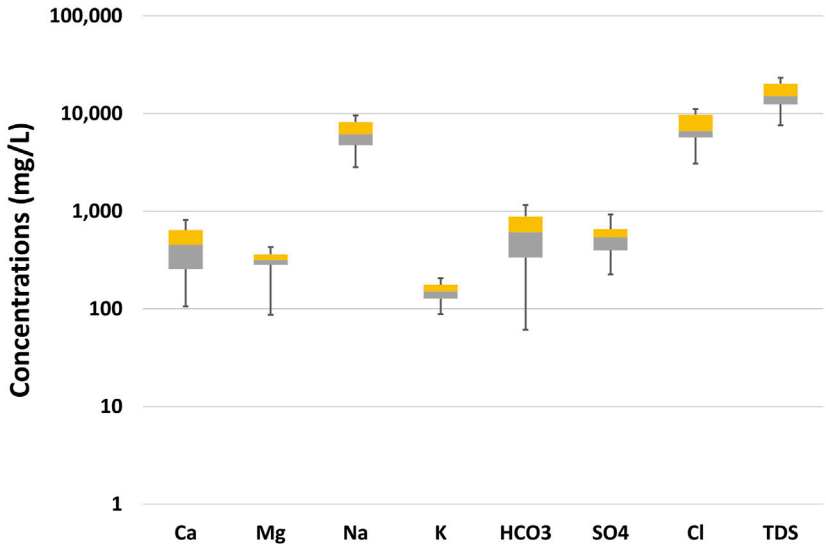

FIGURE 6
Box plots for the hydrogeochemical characteristics of the collected groundwater samples.

chloride concentration, and total dissolved solids concentration. Geophysical approaches are being considered as an alternative to these conventional methods to detect the hydrogeological structure of aquifers and monitor the presence of salt water in coastal aquifers (Polemio and Zuffianò, 2020). These methods can be used for monitoring temporal variations in groundwater levels for

TABLE 1 Hydrochemical analysis of the collected samples from the shallow aquifer and sea.

	Lat	Long	Ca	Mg	Na	K	HCO_3	CO_3	SO_4	Cl	NO_3	TDS
			mg/L									
GW1	31° 4′15.60″N	32°30′17.50″E	600	330	6,341	158	61	Nil	554	7,550	Nil	15,594
GW2	31° 4′20.40″N	32°30′13.80″E	706	361	7,156	174	122	Nil	540	8,541	Nil	17,600
GW3	31° 4′56.00″N	32°30′30.40″E	682	362	8,120	179	183	Nil	625	9,697	Nil	19,848
GW4	31° 4′49.80″N	32°30′21.80″E	283	310	5,113	151	244	Nil	929	6,199	Nil	13,229
GW5	31° 3′42.00″N	32°27′40.00″E	264	300	5,671	140	305	Nil	478	6,177	Nil	13,335
GW6	31° 3′36.00″N	32°27′52.00″E	306	290	4,326	142	366	Nil	506	5,435	Nil	11,371
GW7	31° 3′30.50″N	32°28′22.00″E	222	406	9,512	200	427	Nil	224	11,087	Nil	22,078
GW8	31° 3′33.00″N	32°28′23.00″E	814	300	5,114	121	488	Nil	298	6,262	Nil	13,397
GW9	31° 4′3.50″N	32°25′57.00″E	525	277	3,236	88	549	Nil	479	4,342	Nil	9,496
GW10	31° 5′28.00″N	32°30′36.00″E	155	259	4,681	124	610	Nil	325	5,473	Nil	11,627
GW11	31° 5′29.00″N	32°30′36.00″E	161	265	4,346	123	671	Nil	300	5,460	Nil	11,326
GW12	31° 5′26.00″N	32°30′34.00″E	488	320	6,128	148	732	Nil	722	6,634	Nil	15,172
GW13	31° 4′55.00″N	32°30′3.00″E	708	416	8,251	184	793	Nil	674	9,781	Nil	20,807
GW14	31° 5′3.00″N	32°30′39.00″E	806	430	9,193	206	854	Nil	655	10,910	Nil	23,054
GW15	31° 4′23.00″N	32°30′31.00″E	453	327	6,117	152	915	Nil	652	8,168	Nil	16,784
GW16	31° 3′15.50″N	32°30′15.00″E	577	361	9,530	188	976	Nil	720	10,866	Nil	23,218
GW17	31° 3′42.00″N	32°29′57.00″E	445	315	4,780	158	1,037	Nil	587	5,914	Nil	13,236
GW18	31° 5′4.20″N	32°30′10.00″E	247	241	8,600	130	1,098	Nil	470	9,705	Nil	20,491
GW19	31° 7′17.00″N	32°25′9.00″E	106	87	2,810	88	1,159	Nil	242	3,067	Nil	7,559
Max			814	430	9,530	206	1,159	0	929	11,087	0	23,218
Min			106	86	2,810	88	61	0	224	3,067	0	7,558
Average			449	313	6,264	150	610	0.00	525	7,435	0	15,748
Seawater	31° 4′53.43″N	32°33′3.03″E	930	325	11,850	157	151	35	3,012	18,211	20	40,820

sustainable water resource management (Essam et al., 2020). Even though several geophysical techniques can be used to describe coastal regions, the electrical resistivity method is more closely associated with pore water salinity. Many articles emphasize the use of electrical resistivity method for the analysis of seawater intrusion events and the characterization of coastal environments (Aladejana et al., 2020; Hasan et al., 2020).

The coastal aquifer of Port Said is undergoing an excessive extraction in the context of climate change, resulting in a probable seawater intrusion. Such a situation requires an investigation of groundwater salinization in terms of sources and processes (Argamasilla et al., 2017; Aretouyap et al., 2020). Recently, the Egyptian government declared East Port Said as an industrial area to host a set of projects. Therefore, in addition to anterior studies addressing the Port Said geological setting (El-Asmar, 1999; Goodfriend and Stanley, 1999; Stanley, 2005), subsidence (Stanley et al., 2008) and tectonic activities (Sneh and Weissbrod, 1973; Neev, 1977; Stanley et al., 2008), numerous other ones were conducted (Stanley and Toscano, 2009; Quintanar et al., 2013; Pennington et al., 2017). Moreover, satellite imagery and geographic information systems (GIS) were used for monitoring the rapid changes in (LU/LC), and assessing risks along East Port Said due to anthropogenic interference (Kaiser, 2009; El-Asmar et al., 2015; Gaber et al., 2016; Arnous et al., 2017). Many authors have studied the geo-environmental hazards, including in waterlogged areas, increased soil salinity, coastal erosion, and dune sand encroachment, which affect the study area and cause severe land degradation, which threat different developmental plans (Dai et al., 2001; Arnous et al., 2017; Moubarak et al., 2021).

Although there are numerous studies in the East Port Said area, the groundwater quality and its degradation drivers have not yet been meticulously investigated. However, this is relevant for groundwater resources management. Hence, the goal of the current study is to identify anthropogenic activities that have an impact on groundwater resources in the shallow aquifer in East Port Said, Egypt. To achieve that, water chemistry and geophysical technique are combined with remote sensing datasets (such as multi-temporal Landsat images) between 1984 and 2015. Fish farms and vegetation changes in the

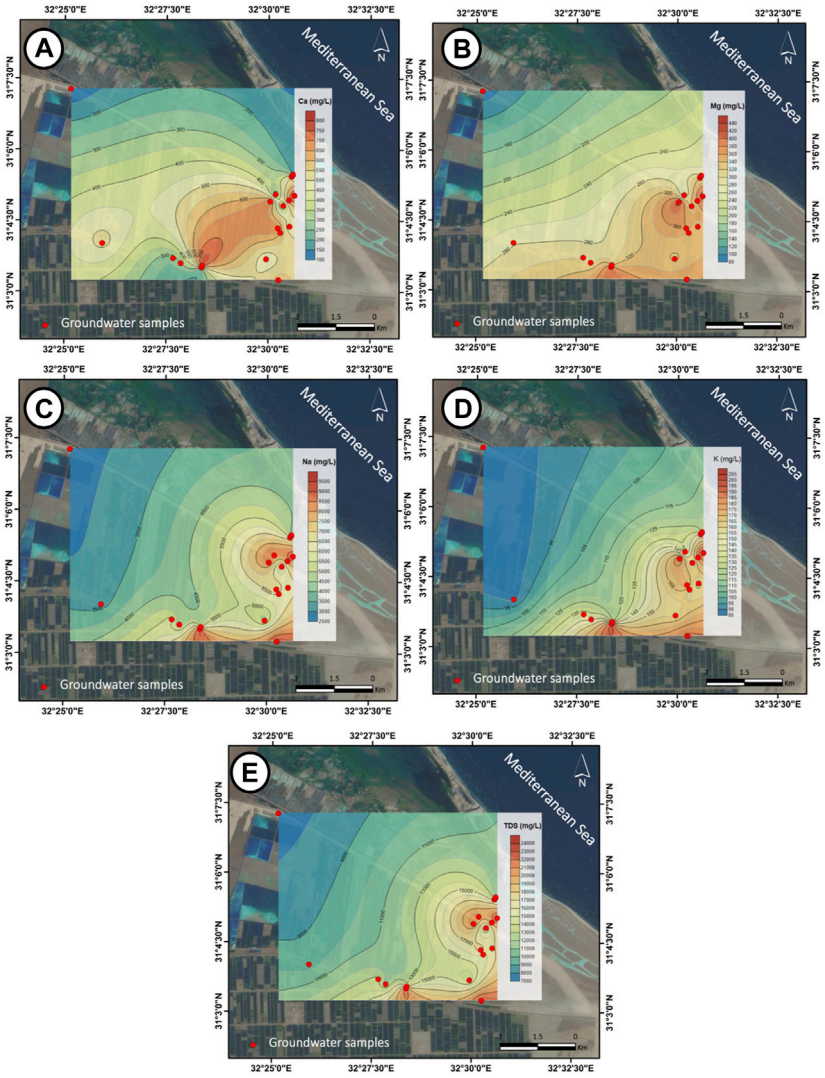

FIGURE 7
Maps of the spatial distribution of major cations: **(A)** Ca^{2+}, **(B)** Mg^{2+}, **(C)** Na^{+}, **(D)** K^{+}, and **(E)** TDS.

study region were monitored through the analysis of LULC maps. Finally, the potential sources of groundwater degradation were identified using LULC analysis, geophysical interpretation and water quality indices.

2 Study area

The study area is located in the East Port Said governorate on the eastern side of the Nile Delta. The area lies between the longitudes 32°22′–32°34′ E and latitudes 31°02′–31°9′N. It covers an area of about 189 km^2 and extends from the El-Bardawil Lagoon eastward, the Suez Canal westward, El Qantara-El Arish asphaltic road in the south to the Mediterranean Sea at the north (Figure 1A). The area is mainly characterized by low elevation and flat terrain of about 5 m above sea level. In contrast, some western, southern, and eastern areas are higher than 5 m (Figure 1D).

Geologically, the study area is represented by the old deltaic plain of the ancient Pellusic Nile branch that has been traced at the east of the Suez Canal between El-Baqar canal and Tell El-Farama with the two marking distributaries that branched northward (Sneh et al., 1975). The study area is an integral part of the ancient Nile Delta system (Stanley, 1988). It is entirely covered by Holocene and Pleistocene sediments of littoral, alluvial, and aeolian origin (Figure 1B), which show variations in their textures, and compositions and range from unconsolidated sands to salinized silt and clay of chemical and biochemical origins (Dewidar and Frihy, 2003).

According to geological studies (Geriesh et al., 2015), three different aquifer types can be distinguished:

1. The lower aquifer forms the main aquifer in the southern sector of the research area. It is semi-confined, 80 m thick, and composed of gravelly sands. It corresponds to the early Pleistocene sequence.

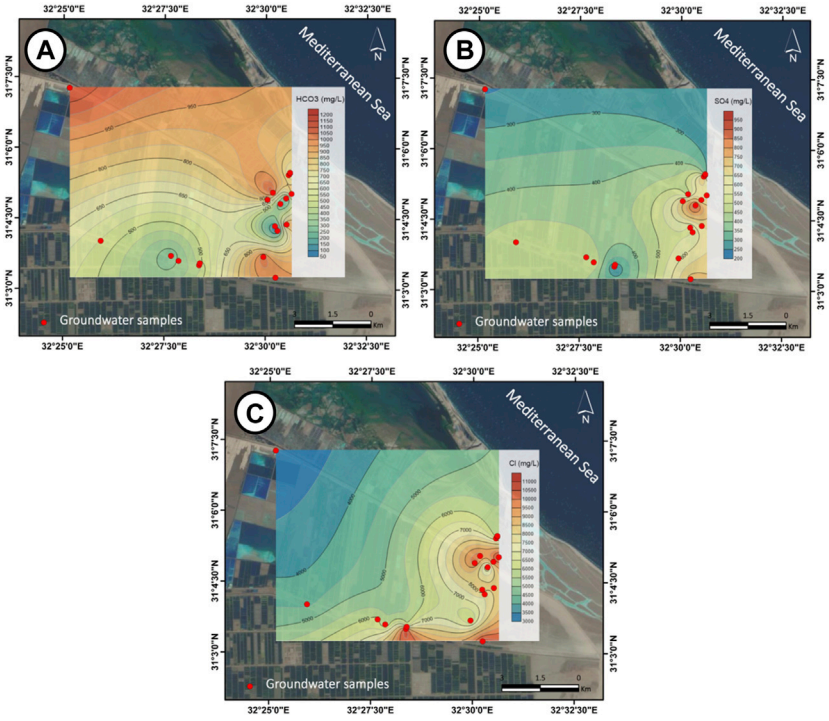

FIGURE 8
(A) Maps of the spatial distribution of major anions, **(A)** HCO_3^-, **(B)** SO_4^{2-}, **(C)** Cl^-

2. The intermediate aquifer is above the main aquifer along the northern sector. It is semi-confined, 15 m thick, and belongs to the late Pleistocene.
3. The upper low permeable aquifer, which covers the El-Tina Plain area and has a thickness of around 33 m, is considered unconfined and corresponds to the late Pleistocene-Holocene. It occasionally forms an aquitard layer along the El-Tina plain's center core.

The northern sector crosses through lowland areas (+/-1 masl.). It is bounded by old deltaic loamy sand deposits deposited in an extended morpho-tectonic basin. Such deposits contain brackish to saline groundwater. Water salinity increases with depth, reflecting the occurrence of two groundwater horizons. The deeper one is probably fossil water that may have been affected by the Plio-Pleistocene fluviomarine wet periods with long resident time. While the less saline shallow groundwater floats over those mentioned above brackish, the deeper one is due to density variations and probably from recent freshwater recharge from the El-Salam canal irrigation system. Figure 2 shows the geological cross-section along the study area, mainly composed of sandstone layers sometimes intercalating with clay lenses and clay.

3 Materials and methods

In this research, anthropogenic activities were identified to determine their impacts on groundwater quality in the shallow aquifer in East Port Said, Egypt by integrating remote sensing, geophysical method, and water chemistry.

- Remote sensing images (from 1984 to 2015) with field validation are used to identify the new features (fish farms and vegetation) that occurred in 2015.
- The geophysical method is used to determine the subsurface lithology and groundwater salinity depending on the measured resistivity values.
- Hydrochemical analysis of groundwater samples identified the origin and hydrogeochemical processes that have an impact on groundwater.

3.1 Remote sensing technique

Remote sensing methods are thought to be the greatest way to monitor localized changes and investigate novel phenomena on the surface of the Earth and even other planets. Using satellite remote sensing images, it is possible to produce precise and timely geographic data describing changes in LU/LC.

3.1.1 Characteristics of the used satellite dataset

East Port Said is represented by two Landsat-5 and Landsat-8 images that were used. The Landsat-5 image was acquired on 2 July 1984, and is characterized by the path/row 175/038. This ancient time highlights the research area's previous conditions through its surface features. While the latest Landsat-8 image with the path/row 175/038 was acquired on 24 July 2015. This present time was chosen since it coincides with groundwater sample collection and fieldwork. These satellite imageries were downloaded for free from the Earth Explorer USGS website (http://earthexplorer.usgs.gov).

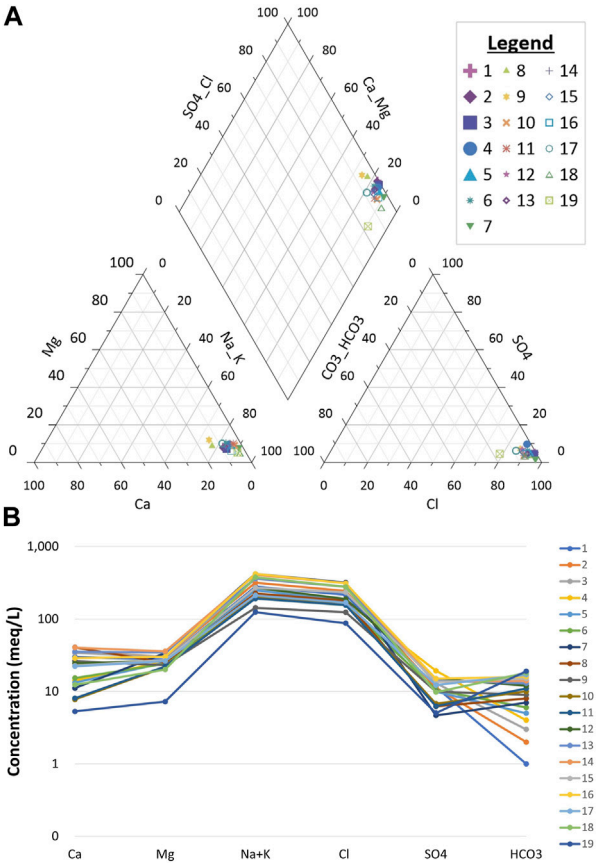

FIGURE 9
(A) Piper diagram for water types determination, **(B)** Scholar's diagram of groundwater samples.

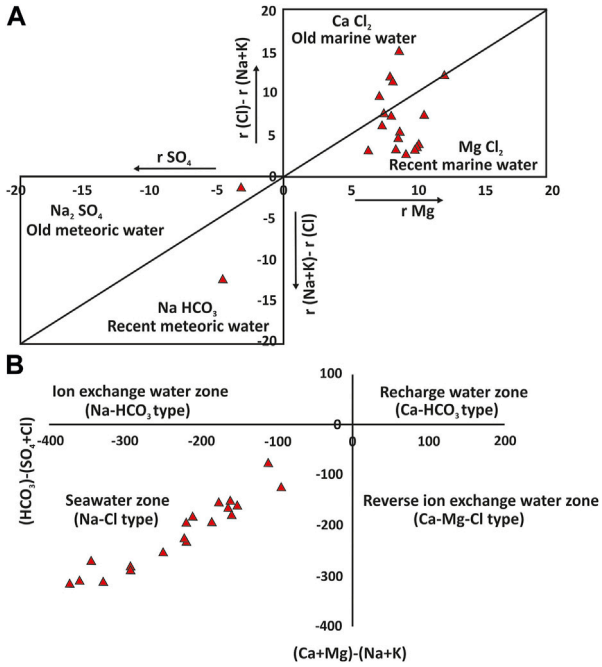

FIGURE 10
(A) Sulin's diagram showing the genetic types of the groundwater samples, **(B)** Chadha's plot of groundwater chemistry showing the hydrogeochemical processes.

3.1.2 Landsat data processing

A variety of image processing techniques were developed to improve the image and help distinguish the various types of geology and land cover. Stacking, clipping, false color composition (FCC), and supervised classification are some of these techniques. The FCC Landsat-5 image was created using bands 5, 3, and 2. Landsat-8 image, on the other hand, was created using bands 7, 5, and 3 in RGB, while the FCC. Landsat-5 and Landsat-8 images can be divided into 4 and 6 groups according to supervised classification using the maximum likelihood classifier (MLC) for parametric input data and field investigation. Figures 3A–D shows the surface features such as sabkha, clay, fish farms, and vegetation that were widespread in the study region in 2015 during the field investigation to ensure high accuracy outputs from satellite image processing.

3.2 Geophysical survey

The electrical resistivity technique is one of the most popular techniques that can be used for subsurface investigation through detecting Earth resistivity by injecting a direct current (DC) signal into the subsurface and measuring the potentials (voltages) that are formed there. Using the information collected, the electrical characteristics of the Earth can be deduced (Sundararajan et al., 2012). The theory and applications of this strategy in groundwater investigations have been well described (Zohdy, 1965; 1975; Bhattacharya and Patra, 1968; Parasnis, 1973; Arétouyap et al., 2019; Abdelfattah et al., 2021).

In this study, the geoelectric survey was carried out using a one-dimensional Schlumberger array with a maximum current electrode spacing (AB) of 600 m to reasonably reach deep depths. Six resistivity soundings were completed in the study region, as indicated in Figure 3F. To comprehend the underlying sequences and identify the various aquifer layers, field measurements were conducted starting from 2 m between the current's poles and increasing up to 600 m. To record changes in ground resistance values, the Syscal R-2 system (Figure 3E), which sends an electrical current through the Earth, was used. Finally, the true resistivity values for the various geoelectric layers were calculated using Ipi2Win software by correlating the apparent resistivity of each VES with the underlying geological model received from a nearby drilled well.

3.3 Hydrogeochemical analysis of groundwater samples

A total of 19 groundwater samples from shallow wells along the study area were collected on July 2015 (Figure 1C). One surface water sample from the Mediterranean Sea was collected for reference use. These samples were collected in pre-washed and clean 1,000-ml polyethylene plastic bottles and stored in a refrigerator at 4°C. The chemical analysis followed the standard methods advised by

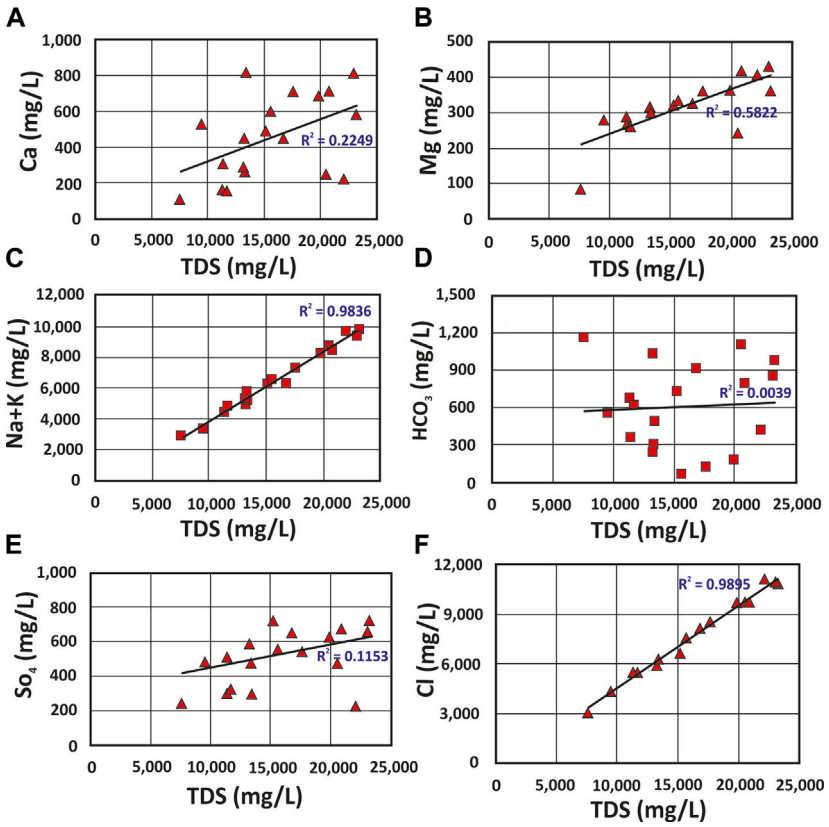

FIGURE 11
TDS–Ion relationships: **(A)** Ca-TDS, **(B)** Mg-TDS, **(C)** Na+K-TDS, **(D)** HCO_3-TDS, **(E)** SO_4-TDS and **(F)** Cl-TDS.

(APHA, 2005). The chemical analyses included the major cations (Na, K, Ca, Mg) and the anions (HCO_3, CO_3, Cl, and NO_3) and were conducted by using Inductively Coupled Plasma (ICP) at the Chemical War Institute of the Armed Forces, Cairo, Egypt. The Total dissolved solids (TDS) of the groundwater samples were measured *in situ*. Different graphs, such as Piper, Scholler, sulin, and Chadha graphs, were plotted to show the effect of seawater intrusion on the hydrogeochemical analysis of groundwater (Piper, 1944; Subrahmanyam and Yadaiah, 2001; Hiscock, 2005). Besides that, the ratios were calculated by SPSS software, including rNa/rCl, rCl/r (HCO_3+CO_3), and rSO_4/rCl. These ratios prove the salinity levels were mostly influenced by the ions present in seawater (Na and Cl), determine whether or not the salinity source is seawater, and the hydrogeochemical processes that have an impact on groundwater (Piper, 1944; Hem, 1989; Subrahmanyam and Yadaiah, 2001; Hiscock, 2005; Nwankwoala and Udom, 2011; Zakari et al., 2014; Abdelfattah et al., 2023; Gamal et al., 2023).

4 Results and discussion

The results analyzed the effect of anthropogenic activities that were detected from LULC maps in the study area from 1984 to 2015, then investigated their effect on groundwater resources in terms of quality and deterioration drivers. The chemical analysis of the groundwater sampled depicts the phenomenon of seawater intrusion.

4.1 Land cover units

It is clear from the processed satellite image that a change occurred in the study area over the investigation period. In 1984 (Figures 4A, B), the main units of land cover were sabkha (65%), clay (30.5%), wetlands (2.5%) around El-Mallaha Lake, and sand toward the east (2%). After the El-Salam Canal was dug up and the mega-project of development communities aimed at land reclamation and cultivation east of the Suez Canal was established, the development operations started later in 1991 and were almost finished by the year 2000. The fish farm and vegetation, which covered 12.5 and 37.8 km^2, respectively, were clear evidence of the development operations in 2015 (Figure 4C). These human activities relied on groundwater as a primary source of water.

For evaluating the classification precision, more than 300 reference points that are completely different from the points utilized in supervised classifications and indicating the defined classes were employed. These reference points were mostly selected during the field trip and the rest from Google Earth. 70 reference points for each class are therefore sufficient for assessing the categorization accuracy of the research region. An error matrix was generated by comparing the labels that were placed on each supervised classification map to the labels in the reference dataset after evaluating the chosen points in each reference dataset. Each class's user and producer accuracies were determined as well as the overall map accuracy. The two produced classification images

TABLE 2 Ionic ratios of the collected samples.

	Na/Cl	SO_4/Cl	Cl/HCO_3
GW1	1.28	0.05	215.7
GW2	1.27	0.05	122.0
GW3	1.27	0.05	92.4
GW4	1.26	0.11	44.3
GW5	1.4	0.06	35.3
GW6	1.21	0.07	25.9
GW7	1.31	0.01	45.3
GW8	1.24	0.03	22.4
GW9	1.13	0.08	13.8
GW10	1.3	0.04	15.6
GW11	1.21	0.04	14.2
GW12	1.41	0.08	15.8
GW13	1.28	0.05	21.5
GW14	1.28	0.04	22.3
GW15	1.14	0.06	15.6
GW16	1.33	0.05	19.4
GW17	1.23	0.07	9.9
GW18	1.35	0.04	15.4
GW19	1.39	0.06	4.6
Average	1.28	0.05	40.6
Minimum	1.14	0.01	4.6
Maximum	1.41	0.08	215.7
Seawater	0.65	0.15	120.6

from 1984 to 2015 have accuracy percentages of 95.7% and 94.8%, respectively. As a result, the produced classified maps were accurate.

4.2 Interpretation of resistivity method

The subsurface succession of the geoelectric layers in the research area was ascertained using a quantitative and qualitative interpretation of the field data from the six geoelectrical soundings. The results show that there is a general class of curve called K-HQA-HK. IPI2Win program explained how the mathematical model of the field measurements should be interpreted. Figure 5 shows some examples of the processed VES soundings and their geoelectric layers. The sedimentary sequence was vertically made up of a set of geoelectric layers (A, B, and C) as well as the surface layer, with their data arranged as follows from top to bottom:

1. The first surface layer (A): This layer of modern sediments, which extends from the Earth's surface to a depth of about 0.5–1.8 m, is almost high resistance for the lower layers, where the resistance ranges from 20 to 80 Ω·m.
2. The second layer (B): The second layer is thicker than the surface layer above it and can reach depths of 9–25 m. It can range in thickness from 1.7 to 8 m and has a very low electrical resistance of less than 1 Ω·m, which could indicate salt-saturated clay deposits.
3. The third layer (C), which consists of mud and sand saturated with seawater and extends beneath the second layer, carries salt water to depths that have not yet been reached due to the discontinuation of electric current layers. Its electrical resistance is between 6 and 18 Ω·m. It resembles a stratum of salt-water-filled coarse sandstone.

The substantial saline water content present in the shallow subsurface layers had a significant impact on the resistivity approach. It is crucial to be completely familiar with the study region because its geological and geophysical characteristics, particularly in coastal environments, could support one method over another (Abdelfattah et al., 2021).

4.3 Groundwater quality dataset

4.3.1 Spatial distribution of ions

Interpreting the hydrogeochemical parameters helps to understand the hydrogeological conditions and aid in decisions concerning water use. Table 1 displays the results of the chemical analysis of groundwater samples collected in the study area. It appears that local groundwater is very saline (Winslow and Kister, 1956), due to high concentrations of TDS with values varying from 7,558 to 23,218 mg/L with an average of 15,748 mg/L (Table 1). In addition, the minimum TDS values of groundwater were recorded in the western part of the study area. The salinity has increased toward the eastern and southern parts due to the overexploiting of groundwater resources for fish farms and vegetation (Figure 7E). Leaching from drains, agricultural irrigation, and human activity may be responsible for the high salinity in the shallow groundwater zone (Khalil et al., 2021).

The concentrations of major ions in groundwater samples prove that Na^+ is the dominant cation (Figure 6), with concentration values ranging from 2,800 to 9,530 mg/L. Ca^{2+} and Mg^{2+} are the

TABLE 3 Contamination by seawater based on rCl/r (HCO_3+CO_3) ratio.

rCl/rHCO_3 + CO_3	Water class	Percent (no. of samples)
2.8–6.6	Injuriously contaminated	5.2% (1)
6.6–15.5	Highly contaminated	21.05% (4)
>15.5	Severely contaminated	73.6% (14)

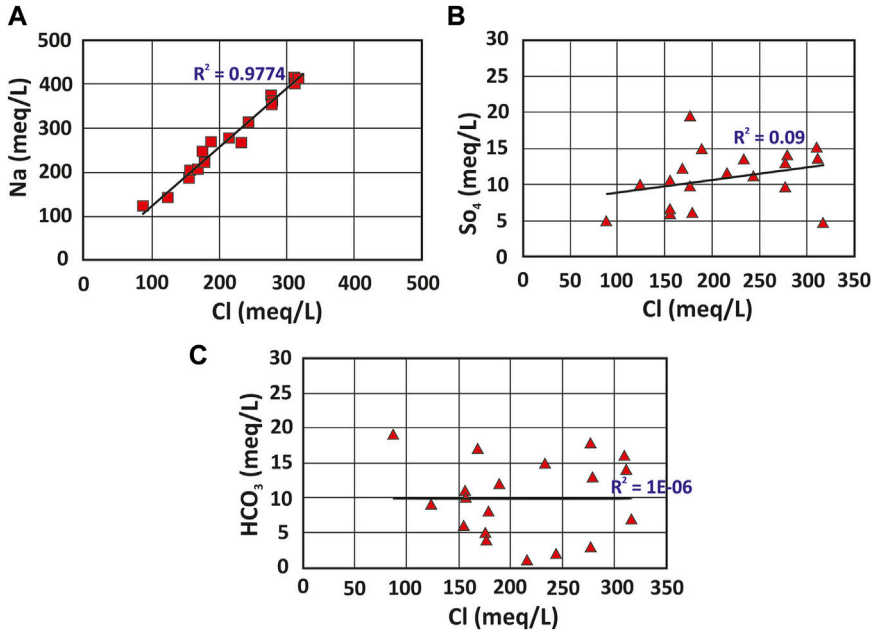

FIGURE 12
Ion relationships: **(A)** Na-Cl, **(B)** SO_4-Cl, **(C)** HCO_3-Cl.

second most dominant cations, with an average concentration of 450 and 313 mg/L, respectively. K has the lowest concentration values ranging from 88 to 206 mg/L. Cl^- is the dominant anion with concentration values from 3,000 to 11,000 mg/L and HCO_3^- is the second one with concentrations ranging from 60 to 1,150 mg/L. SO_4^{2-} is the ion with the lowest concentration values, ranging from 240 to 920 mg/L. The spatial distributions of cations (Na^+, Ca^{2+}, Mg^{2+}, K^+) (Figures 7A–D) and anions (SO_4^{2-} and Cl^-) show an increasing trend toward the eastern and southern parts of the study area (Figures 8B, C). Unlike all analyzed ions (cations and anions), bicarbonate concentrations increase toward the northwestern side of the study area with a value of 1,160 mg/L (Figure 8A).

High salinity, the dominance of Na^+ and Cl^- as well as their spatial distribution demonstrate that overexploiting of groundwater may have contributed to the impact of seawater intrusion. The water table decreases significantly as a result, and the necessity for seawater to invade the land increases. Therefore, seawater intrusion affects the spatial distribution of major cations and anions of the groundwater.

4.3.2 Groundwater type

The Piper diagram is one of the important representations for understanding and evaluating the hydrogeochemical characteristics of groundwater. Both the Piper diagram and the Scholler diagram show that Na is the major cation and Cl is the major anion in all samples with high values of TDS and Na-Cl type (Na > Ca > Mg and Cl > SO_4 > HCO_3), which confirm the impact of seawater intrusion on the shallow aquifer (Figures 9A, B).

4.3.3 Salinization processes

The hydrogeochemical processes occur when the groundwater moves toward an equilibrium state in major ion concentrations. Some hydrogeological presentations (Sulin and Chadha plots) can be used to determine such hydrogeochemical processes. In this study, Sulin's diagram shows the recent marine water ($MgCl_2$) genetic type for most of the groundwater samples (Figure 10A). While only 4 groundwater samples show old marine water type ($CaCl_2$), and two samples were located equally in a recent meteoric water type ($NaHCO_3$) and old meteoric water type (Na_2SO_4). Therefore, Chadha's plot confirms the influence of seawater intrusion into the aquifer because all samples have been located in the seawater zone (Figure 10B).

4.3.4 Ions relations

To understand the origin of the salts and the hydrogeochemical processes impacting the groundwater, the relationship between these different major ions should be considered. TDS vs. major ions are examples of these relationships (Figure 11). The following notes can be extracted from these relations:

1. The seawater intrusion is the major source of salinity due to the higher correlation coefficient values of r^2= 0.98 and 0.98 between the TDS/Na and TDS/Cl, respectively, and clustered parallel to the trend line (Figures 11C, F).
2. The predominance of ion exchange and carbonate minerals deposition is clear from the relationships between TDS/Ca and TDS/Mg, which show low correlation coefficient values of r^2= 0.22 and 0.58, respectively (Figures 11A, B).
3. Carbonate ions are not of primary origin because the TDS/HCO_3 relationship shows a very low correlation coefficient r^2= 0.003 (Figure 11D).

These ratios confirm that the salinity values were mostly influenced by the concentrations of ions in the seawater (Na and Cl). To

confirm that the salinity source is from seawater, ionic ratios like rNa/rCl, rCl/r (HCO_3+CO_3), and rSO_4/rCl were calculated and plotted on a graph (Tables 2, 3; Figure 12).

Some limitations must be taken into account in future research, even though integrated approaches have been utilized in the study region to examine the impact of human activities and seawater intrusion on the shallow coastal aquifer. For instance, the research area's groundwater sample distribution is not ideal, despite the application of geophysics techniques to address this shortcoming. The employment of additional geophysical techniques, such as the time domain electromagnetic approach, can penetrate further depths and are not affected by the highly salinized groundwater. In addition to doing advanced testing on groundwater samples, such as isotopic analysis, to determine the extent to which seawater intrusion has affected the research area.

5 Conclusion

This paper describes the origin of salinity and the geochemical processes that resulted from human activities in the shallow Quaternary coastal aquifer of East Port Said. This research was conducted using a combined remote sensing, hydrogeological, geophysical, and hydrochemical approach. LULC maps show that drastic surface changes occurred in the study area from 1984 to 2015. In 1984, the study area was completely covered by sabkha and other surface features such as clay, sand, and wetlands. However, by 2015, significant changes occurred, where new features such as fish farms and vegetation cover appeared and expanded to reach their area of 12.5 and 37.8 km^2. The resistivity technique was employed to evaluate water quality. This approach was significantly impacted by high saline water content, which led to the discontinuation of electric current layers. Additionally, a total of 19 groundwater samples were collected from the aforementioned aquifer and one sample from the sea. The collected groundwater samples are very saline due to a high concentration of TDS with an average of 15,700 mg/L towards the places either near the coastline (north part) or close to the places where groundwater is over-extracted (south part). Moreover, the hydrogeochemical analysis of groundwater samples shows that Na+ and Cl^- are the dominant ions with Na-Cl water type, which is confirming the influence of seawater intrusion. As well as some plots (Sulin and Chadha plots) were presented and showed all samples fall in the zone of seawater intrusion. The ionic ratios (TDS vs. major ions) confirm that the TDS was largely influenced by Na^+ and Cl^-. Finally, (rNa/rCl, rCl/r (HCO_3+CO_3), and rSO_4/rCl) were calculated and used for correlation analysis to obtain evidence for seawater intrusion. Therefore, these new developmental projects cause a draw-down in the groundwater table due to continuous pumping and consequently caused seawater intrusion. All results obtained in this investigation confirm that the main source of salinity in the shallow groundwater coastal aquifer in the study area is related to seawater intrusion. An improved understanding of water sources, especially in shallow coastal aquifers in arid regions, could enhance the assessment of water contamination sources and the ensuing delivery of useful data for the management of water resources and sustainability strategies. Despite the use of several techniques to demonstrate the influence of seawater in the coastal aquifer in the research region, we will still need to validate this event in the future by conducting additional geophysical techniques and isotopic analyses for groundwater samples.

Data availability statement

The original contributions presented in the study are included in the article/supplementary material, further inquiries can be directed to the corresponding author.

Author contributions

All authors listed have made a substantial, direct, and intellectual contribution to the work and approved it for publication.

Funding

Princess Nourah Bint Abdulrahman University Researchers Supporting Project number (PNURSP2023R243), Princess Nourah Bint Abdulrahman University, Riyadh, Saudi Arabia.

Conflict of interest

The authors declare that the research was conducted in the absence of any commercial or financial relationships that could be construed as a potential conflict of interest.

Publisher's note

All claims expressed in this article are solely those of the authors and do not necessarily represent those of their affiliated organizations, or those of the publisher, the editors and the reviewers. Any product that may be evaluated in this article, or claim that may be made by its manufacturer, is not guaranteed or endorsed by the publisher.

References

Abdalla, F., Al-Turki, A., and Al Amri, A. (2015). Evaluation of groundwater resources in the southern tihama plain, Saudi Arabia. *Arab. J. Geosci.* 8, 3299–3310. doi:10.1007/s12517-014-1401-3

Abdalla, F. (2016). Ionic ratios as tracers to assess seawater intrusion and to identify salinity sources in Jazan coastal aquifer, Saudi Arabia. *Arab. J. Geosci.* 9, 40–12. doi:10.1007/s12517-015-2065-3

Abdelfattah, M., Abu-Bakr, H. A.-A., Mewafy, F. M., Hassan, T. M., Geriesh, M. H., Saber, M., et al. (2023). Hydrogeophysical and hydrochemical assessment of the northeastern coastal aquifer of Egypt for desalination suitability. *Water* 15, 423. doi:10.3390/w15030423

Abdelfattah, M., Gaber, A., Geriesh, M. H., and Hassan, T. M. (2021). Investigating the less ambiguous hydrogeophysical method in exploring the shallow

coastal stratified-saline aquifer: A case study at west port Said coast, Egypt. *Environ. Earth Sci.* 80, 1–14. doi:10.1007/s12665-021-09442-8

Ahmed, M. A., Abdel Samie, S. G., and Badawy, H. A. (2013). Factors controlling mechanisms of groundwater salinization and hydrogeochemical processes in the Quaternary aquifer of the Eastern Nile Delta, Egypt. *Environ. Earth Sci.* 68, 369–394. doi:10.1007/s12665-012-1744-6

Aladejana, J. A., Kalin, R. M., Sentenac, P., and Hassan, I. (2020). Hydrostratigraphic characterisation of shallow coastal aquifers of Eastern Dahomey Basin, S/W Nigeria, using integrated hydrogeophysical approach; implication for saltwater intrusion. *Geosciences* 10, 65. doi:10.3390/geosciences10020065

APHA (2005). *APHA standard methods for the examination of water and wastewater.* Stand. methods Exam. water wastewater. Washington, DC Am: Public Heal. Assoc.

Aretouyap, Z., Billa, L., Jones, M., and Richter, G. (2020). Geospatial and statistical interpretation of lineaments: Salinity intrusion in the kribi-campo coastland of Cameroon. *Adv. Sp. Res.* 66, 844–853. doi:10.1016/j.asr.2020.05.002

Arétouyap, Z., Bisso, D., Méli'i, J. L., Njandjock Nouck, P., Njoya, A., and Asfahani, J. (2019). Hydraulic parameters evaluation of the Pan-African aquifer by applying an alternative geoelectrical approach based on vertical electrical soundings. *Geofísica Int.* 58, 113–126.

Argamasilla, M., Barberá, J. A., and Andreo, B. (2017). Factors controlling groundwater salinization and hydrogeochemical processes in coastal aquifers from southern Spain. *Sci. Total Environ.* 580, 50–68. doi:10.1016/j.scitotenv.2016.11.173

Arnous, M. O., El-Rayes, A. E., and Helmy, A. M. (2017). Land-use/land-cover change: A key to understanding land degradation and relating environmental impacts in northwestern sinai, Egypt. *Environ. Earth Sci.* 76, 1–21. doi:10.1007/s12665-017-6571-3

Baker, T. J., and Miller, S. N. (2013). Using the Soil and Water Assessment Tool (SWAT) to assess land use impact on water resources in an East African watershed. *J. Hydrol.* 486, 100–111. doi:10.1016/j.jhydrol.2013.01.041

Bhattacharya, A., and Patra, H. P. (1968). *Direct current geoelectric prospecting.*

Brown, D., Polsky, C., Bolstad, P. V., Brody, S. D., Hulse, D., Kroh, R., et al. (2014). *Land use and land cover change.* Richland, WA (United States): Pacific Northwest National Lab PNNL.

Chávez, R. O., Clevers, J., Decuyper, M., De Bruin, S., and Herold, M. (2016). 50 years of water extraction in the Pampa del Tamarugal basin: Can Prosopis tamarugo trees survive in the hyper-arid Atacama Desert (Northern Chile)? *J. Arid. Environ.* 124, 292–303. doi:10.1016/j.jaridenv.2015.09.007

Chen, J., Chen, J., Liao, A., Cao, X., Chen, L., Chen, X., et al. (2015). Global land cover mapping at 30 m resolution: A POK-based operational approach. *ISPRS J. Photogramm. Remote Sens.* 103, 7–27. doi:10.1016/j.isprsjprs.2014.09.002

Chidambaram, S., Anandhan, P., Prasanna, M. V., Thivya, C., Thilagavathi, R., Sarathidasan, J., et al. (2014). Hydrochemistry of groundwater in a coastal region and its repercussion on quality, a case study—thoothukudi district, Tamil nadu, India. *Arab. J. Geosci.* 7, 939–950. doi:10.1007/s12517-012-0794-0

Dai, F. C., Lee, C. F., and Zhang, X. H. (2001). GIS-Based geo-environmental evaluation for urban land-use planning: A case study. *Eng. Geol.* 61, 257–271. doi:10.1016/s0013-7952(01)00028-x

De Filippis, G., Foglia, L., Giudici, M., Mehl, S., Margiotta, S., and Negri, S. L. (2016). Seawater intrusion in karstic, coastal aquifers: Current challenges and future scenarios in the Taranto area (southern Italy). *Sci. Total Environ.* 573, 1340–1351. doi:10.1016/j.scitotenv.2016.07.005

Dewidar, K. M., and Frihy, O. E. (2003). Thematic Mapper analysis to identify geomorphologic and sediment texture of El Tineh plain, north-Western coast of Sinai, Egypt. *Int. J. Remote Sens.* 24, 2377–2385. doi:10.1080/01431160110115807

El-Aassar, A. H. M., Hussien, R. A., Mohamed, F. A., Oterkus, S., and Oterkus, E. (2023). Appraisal of surface–groundwater anthropogenic indicators and associated human health risk in El Sharqia Governorate. Egypt: *J. Water Health.*

El-Asmar, H. M. (1999). Late Holocene stratigraphy and lithofacies evolution of the Tineh plain Northwestern corner of Sinai, Egypt. *Egypt J. Geol.* 43, 119–134.

El-Asmar, H. M., Taha, M., El-Kafrawy, S. B., and El-Sorogy, A. S. (2015). Control of late Holocene geo-processes on the sustainable development plans of the tineh plain, NW sinai coast, Egypt. *J. Coast. Conserv.* 19, 141–156. doi:10.1007/s11852-015-0377-9

El-Saadawy, O., Gaber, A., Othman, A., Abotalib, A. Z., El Bastawesy, M., and Attwa, M. (2020). Modeling flash floods and induced recharge into alluvial aquifers using multi-temporal remote sensing and electrical resistivity imaging. *Sustainability* 12, 10204. doi:10.3390/su122310204

Elhadj, E. (2004). Camels don't fly, deserts don't bloom: An assessment of Saudi Arabia's experiment in desert agriculture. *Occas. Pap.* 48.

Essam, D., Ahmed, M., Abouelmagd, A., and Soliman, F. (2020). Monitoring temporal variations in groundwater levels in urban areas using ground penetrating radar. *Sci. Total Environ.* 703, 134986. doi:10.1016/j.scitotenv.2019.134986

Farshad, A., Erian, W. F., Zarei Abarghuei, S. H., and Shrestha, D. P. (2002). Towards sustainable use of deserts. *17th WCSS.*

Gaber, A., Geriesh, M. H., Shaheen, S., and El-Fattah, M. A. (2016). Mapping the surface changes in the area of East Port-Said, Egypt using multi-temporal and multi-sensors remote sensing data. *J. Appl. Geol. Geophys.* 4, 19–29. doi:10.9790/0990-0405011929

Gamal, G., Hassan, T. M., Gaber, A., and Abdelfattah, M. (2023). Groundwater quality assessment along the West of New Damietta Coastal City of Egypt using an integrated geophysical and hydrochemical approaches. *Environ. Earth Sci.* 82, 107. doi:10.1007/s12665-023-10762-0

Gebrehiwot, A. B., Tadesse, N., and Jigar, E. (2011). Application of water quality index to assess suitability of groundwater quality for drinking purposes in Hantebet watershed, Tigray, Northern Ethiopia. *ISABB J. Food Agric. Sci.* 1, 22–30.

Geological Survey of Egypt (GSE) (1992). Geological map of sinai, A.R.E. Sheet No. 5, Scale 1:250,000.

Geriesh, M., El-Rayes, A., Gomaa, R., Kaiser, M., and Mohamed, M. (2015). Geoenvironmental impact assessment of El-Salam Canal on the surrounding soil and groundwater flow regime, Northwestern Sinai, Egypt. *Catrina Int. J. Environ. Sci.* 12, 17–29.

Goodfriend, G. A., and Stanley, D. J. (1999). Rapid strand-plain accretion in the northeastern Nile Delta in the 9th century AD and the demise of the port of Pelusium. *Geology* 27, 147–150. doi:10.1130/0091-7613(1999)027<0147:rspait>2.3.co;2

Haddad, G., Szeles, I., and Zsarnoczai, J. S. (2008). *Water management development and agriculture in Syria.*

Hasan, M., Shang, Y., Jin, W., Shao, P., Yi, X., and Akhter, G. (2020). Geophysical assessment of seawater intrusion into coastal aquifers of bela plain, Pakistan. *Water* 12, 3408. doi:10.3390/w12123408

Hegazy, D., Abotalib, A. Z., El-Bastaweesy, M., El-Said, M. A., Melegy, A., and Garamoon, H. (2020). Geo-environmental impacts of hydrogeological setting and anthropogenic activities on water quality in the Quaternary aquifer southeast of the Nile Delta, Egypt. *J. Afr. Earth Sci.* 172, 103947. doi:10.1016/j.jafrearsci.2020.103947

Hem, J. D. (1989). *Study and interpretation of the chemical characteristics of natural water.* Washington, DC: USGS US Geological Survey of Water Supply. Paper 2254.

Hiscock, K. M. (2005). *Hydrogeology–principles and practice.* London. UK: Blackwell Science Ltd.

Houghton, R. A. (1994). The worldwide extent of land-use change. *Bioscience* 44, 305–313. doi:10.2307/1312380

Kaiser, M. F. (2009). Environmental changes, remote sensing, and infrastructure development: The case of Egypt's East Port Said harbour. *Appl. Geogr.* 29, 280–288. doi:10.1016/j.apgeog.2008.09.008

Khalil, M. M., Tokunaga, T., Heggy, E., and Abotalib, A. Z. (2021). Groundwater mixing in shallow aquifers stressed by land cover/land use changes under hyper-arid conditions. *J. Hydrol.* 598, 126245. doi:10.1016/j.jhydrol.2021.126245

Khalil, M. M., Tokunaga, T., and Yousef, A. F. (2015). Insights from stable isotopes and hydrochemistry to the Quaternary groundwater system, south of the Ismailia canal, Egypt. *J. Hydrol.* 527, 555–564. doi:10.1016/j.jhydrol.2015.05.024

Lambin, E. F. (1997). Modelling and monitoring land-cover change processes in tropical regions. *Prog. Phys. Geogr.* 21, 375–393. doi:10.1177/030913339702100303

Loveland, T. R., Reed, B. C., Brown, J. F., Ohlen, D. O., Zhu, Z., Yang, L., et al. (2000). Development of a global land cover characteristics database and IGBP DISCover from 1 km AVHRR data. *Int. J. Remote Sens.* 21, 1303–1330. doi:10.1080/014311600210191

Moubarak, A. H., Arnous, M. O., and El-Rayes, A. E. (2021). Integrated geoenvironmental and geotechnical risk assessment of east Port Said region, Egypt for regional development. *Geotech. Geol. Eng.* 39, 1497–1520. doi:10.1007/s10706-020-01571-4

Moukana, J. A., Asaue, H., and Koike, K. (2013). Co-kriging for modeling shallow groundwater level changes in consideration of land use/land cover pattern. *Environ. Earth Sci.* 70, 1495–1506. doi:10.1007/s12665-013-2235-0

Mukherjee, I., and Singh, U. K. (2021). Characterization of groundwater nitrate exposure using Monte Carlo and Sobol sensitivity approaches in the diverse aquifer systems of an agricultural semiarid region of Lower Ganga Basin, India. *Sci. Total Environ.* 787, 147657. doi:10.1016/j.scitotenv.2021.147657

Napoli, M., Massetti, L., and Orlandini, S. (2017). Hydrological response to land use and climate changes in a rural hilly basin in Italy. *Catena* 157, 1–11. doi:10.1016/j.catena.2017.05.002

Narany, T. S., Ramli, M. F., Aris, A. Z., Sulaiman, W. N. A., and Fakharian, K. (2014). "Assessment of the potential contamination risk of nitrate in groundwater using indicator kriging (in amol–babol plain, Iran)," in From Sources to Solution: Proceedings of the International Conference on Environmental Forensics 2013 (Springer), 273–277.

Neev, D. (1977). The pelusium line—A major transcontinental shear. *Tectonophysics* 38, T1–T8. doi:10.1016/0040-1951(77)90207-4

Nwankwoala, H. O., and Udom, G. J. (2011). Studies on major ion chemistry and hydrogeochemical processes of groundwater in port harcourt city, southern Nigeria. *J. Spat. Hydrol.* 11.

Pal, S. C., Ruidas, D., Saha, A., Islam, A. R. M. T., and Chowdhuri, I. (2022). Application of novel data-mining technique-based nitrate concentration susceptibility

prediction approach for coastal aquifers in India. *J. Clean. Prod.* 346, 131205. doi:10.1016/j.jclepro.2022.131205

Parasnis, D. S. (1973). *Mining geophysics*. Netherlands: Elsevier Publishers.

Pennington, B. T., Sturt, F., Wilson, P., Rowland, J., and Brown, A. G. (2017). The fluvial evolution of the Holocene nile delta. *Quat. Sci. Rev.* 170, 212–231. doi:10.1016/j.quascirev.2017.06.017

Pielke Sr, R. A., Marland, G., Betts, R. A., Chase, T. N., Eastman, J. L., Niles, J. O., et al. (2002). The influence of land-use change and landscape dynamics on the climate system: Relevance to climate-change policy beyond the radiative effect of greenhouse gases. *Philos. Trans. R. Soc. Lond. Ser. A Math. Phys. Eng. Sci.* 360, 1705–1719. doi:10.1098/rsta.2002.1027

Piper, A. M. (1944). A graphic procedure in the geochemical interpretation of water-analyses. *Eos, Trans. Am. Geophys. Union* 25, 914–928. doi:10.1029/tr025i006p00914

Polemio, M., and Zuffianò, L. E. (2020). Review of utilization management of groundwater at risk of salinization. *J. Water Resour. Plan. Manag.* 146, 3120002. doi:10.1061/(asce)wr.1943-5452.0001278

Prabhakar, A., and Tiwari, H. (2015). Land use and land cover effect on groundwater storage. *Model. Earth Syst. Environ.* 1, 45–10. doi:10.1007/s40808-015-0053-y

Quintanar, J., Khan, S. D., Fathy, M. S., and Zalat, A.-F. A. (2013). Remote sensing, planform, and facies analysis of the Plain of Tineh, Egypt for the remains of the defunct Pelusiac River. *Sediment. Geol.* 297, 16–30. doi:10.1016/j.sedgeo.2013.09.002

Ranjpisheh, M., Karimpour Reihan, M., Zehtabian, G. R., and Khosravi, H. (2018). Assessment of drought and landuse changes: Impacts on groundwater quality in Shabestar basin, North of Lake Urmia. *Desert* 23, 9–19.

Rateb, A., and Abotalib, A. Z. (2020). Inferencing the land subsidence in the Nile Delta using Sentinel-1 satellites and GPS between 2015 and 2019. *Sci. Total Environ.* 729, 138868. doi:10.1016/j.scitotenv.2020.138868

Ripken, C., Kotsifaki, D. G., and Chormaic, S. N. (2021). Analysis of small microplastics in coastal surface water samples of the subtropical island of Okinawa, Japan. *Sci. Total Environ.* 760, 143927. doi:10.1016/j.scitotenv.2020.143927

Robertson, W. M., Böhlke, J. K., and Sharp, J. M., Jr (2017). Response of deep groundwater to land use change in desert basins of the Trans-Pecos region, Texas, USA: Effects on infiltration, recharge, and nitrogen fluxes. *Hydrol. Process.* 31, 2349–2364. doi:10.1002/hyp.11178

Saber, A. A., Ullah Bhat, S., Hamid, A., Gabrieli, J., Garamoon, H., Gargini, A., et al. (2022). Chemical quality and hydrogeological settings of the el-farafra oasis (western desert of Egypt) groundwater resources in relation to human uses. *Appl. Sci.* 12, 5606. doi:10.3390/app12115606

Salem, Z. E., Atwia, M. G., and El-Horiny, M. M. (2015). Hydrogeochemical analysis and evaluation of groundwater in the reclaimed small basin of Abu Mina, Egypt. *Hydrogeol. J.* 23, 1781–1797. doi:10.1007/s10040-015-1303-9

Shaki, A. A., and Adeloye, A. J. (2006). Evaluation of quantity and quality of irrigation water at Gadowa irrigation project in Murzuq basin, southwest Libya. *Agric. water Manag.* 84, 193–201. doi:10.1016/j.agwat.2006.01.012

Singh, R. K., Villuri, V. G. K., and Pasupuleti, S. (2022). Evaluation of water quality and risk assessment by coupled geospatial and statistical approach along lower Damodar river. *Int. J. Environ. Sci. Technol.* 1–22, 9549–9570. doi:10.1007/s13762-021-03644-0

Sneh, A., and Weissbrod, T. (1973). Nile delta: The defunct pelusiac branch identified. *Sci. (80-* 180, 59–61. doi:10.1126/science.180.4081.59

Sneh, A., Weissbrod, T., and Perath, I. (1975). Evidence for an Ancient Egyptian Frontier Canal: The remnants of an artificial waterway discovered in the northeastern Nile Delta may have formed part of the barrier called" Shur of Egypt" in ancient texts. *Am. Sci.* 63, 542–548.

Stanley, D. J. (1988). Subsidence in the northeastern nile delta: Rapid rates, possible causes, and consequences. *Sci. (80-* 240, 497–500. doi:10.1126/science.240.4851.497

Stanley, J.-D., Bernasconi, M. P., and Jorstad, T. F. (2008). Pelusium, an ancient port fortress on Egypt's nile delta coast: Its evolving environmental setting from foundation to demise. *J. Coast. Res.* 24, 451–462. doi:10.2112/07a-0021.1

Stanley, J.-D. (2005). Submergence and burial of ancient coastal sites on the subsiding Nile delta margin, Egypt. *Méditerranée. Rev. Géogr. Des. pays méditerranéens/Journal Mediterr. Geogr.*, 65–73. doi:10.4000/mediterranee.2282

Stanley, J.-D., and Toscano, M. A. (2009). Ancient archaeological sites buried and submerged along Egypt's nile delta coast: Gauges of Holocene delta margin subsidence. *J. Coast. Res.* 25, 158–170. doi:10.2112/08-0013.1

Subrahmanyam, K., and Yadaiah, P. (2001). Assessment of the impact of industrial effluents on water quality in Patancheru and environs, Medak district, Andhra Pradesh, India. *Hydrogeol. J.* 9, 297–312. doi:10.1007/s100400000120

Sundararajan, N., Sankaran, S., and Al-Hosni, T. K. (2012). Vertical electrical sounding (VES) and multi-electrode resistivity in environmental impact assessment studies over some selected lakes: A case study. *Environ. Earth Sci.* 65, 881–895. doi:10.1007/s12665-011-1132-7

Switzman, H., Coulibaly, P., and Adeel, Z. (2015). Modeling the impacts of dryland agricultural reclamation on groundwater resources in Northern Egypt using sparse data. *J. Hydrol.* 520, 420–438. doi:10.1016/j.jhydrol.2014.10.064

Tang, L., Liu, J., Zeng, J., Luo, X., Ke, W., Li, C., et al. (2023). Anthropogenic processes drive heterogeneous distributions of toxic elements in shallow groundwater around a smelting site. *J. Hazard. Mat.* 453, 131377. doi:10.1016/j.jhazmat.2023.131377

Taylor, C. A., and Stefan, H. G. (2009). Shallow groundwater temperature response to climate change and urbanization. *J. Hydrol.* 375, 601–612. doi:10.1016/j.jhydrol.2009.07.009

Turner, M. A., Haughwout, A., and Van Der Klaauw, W. (2014). Land use regulation and welfare. *Econometrica* 82, 1341–1403.

Werner, A. D. (2010). A review of seawater intrusion and its management in Australia. *Hydrogeol. J.* 18, 281–285. doi:10.1007/s10040-009-0465-8

Winslow, A. G., and Kister, L. R. (1956). *Saline-water resources of Texas*.

Yoshihara, N., Matsumoto, S., Machida, I., and Uchida, Y. (2023). Deciphering natural and anthropogenic effects on the groundwater chemistry of Nago City, Okinawa Island, Japan. *Environ. Pollut.* 318, 120917. doi:10.1016/j.envpol.2022.120917

Zakari, A., Philippe, N. N., Harlin, E. N., Larissa, M. J., and Alain, L. T. S. (2014). Investigation of groundwater quality control in Adamawa-Cameroon region. *J. Appl. Sci.* 14, 2309–2319. doi:10.3923/jas.2014.2309.2319

Zohdy, A. A. R. (1975). *Automatic interpretation of Schlumberger sounding curves, using modified Dar Zarrouk functions*. US Govt.

Zohdy, A. A. R. (1965). The auxiliary point method of electrical sounding interpretation, and its relationship to the Dar Zarrouk parameters. *Geophysics* 30, 644–660. doi:10.1190/1.1439636